

Collapse and rapid resumption of Atlantic meridional circulation linked to deglacial climate changes

J. F. McManus¹, R. Francois², J.-M. Gherardi³, L. D. Keigwin¹ & S. Brown-Leger²

¹Department of Geology and Geophysics, ²Department of Marine Chemistry and Geochemistry, Woods Hole Oceanographic Institution, Woods Hole, Massachusetts 02543, USA

³Laboratoire des Sciences du Climat et de l'environnement, Domaine de CNRS, 91198 Gif-sur-Yvette, France

The Atlantic meridional overturning circulation is widely believed to affect climate. Changes in ocean circulation have been inferred from records of the deep water chemical composition derived from sedimentary nutrient proxies¹, but their impact on climate is difficult to assess because such reconstructions provide insufficient constraints on the rate of overturning². Here we report measurements of ²³¹Pa/²³⁰Th, a kinematic proxy for the meridional overturning circulation, in a sediment core from the subtropical North Atlantic Ocean. We find that the meridional overturning was nearly, or completely, eliminated during the coldest deglacial interval in the North Atlantic region, beginning with the catastrophic iceberg discharge Heinrich event H1, 17,500 yr ago, and declined sharply but briefly into the Younger Dryas cold event, about 12,700 yr ago. Following these cold events, the ²³¹Pa/²³⁰Th record indicates that rapid accelerations of the meridional overturning circulation were concurrent with the two strongest regional warming events during deglaciation. These results confirm the significance of variations in the rate of the Atlantic meridional overturning circulation for abrupt climate changes.

²³¹Pa and ²³⁰Th are produced in sea water at constant rates from the radioactive decay of dissolved ²³⁵U and ²³⁴U ($\beta_{\text{Pa}} = (2.45 \pm 0.05) \times 10^{-3} \text{ d.p.m. m}^{-3} \text{ yr}^{-1}$; $\beta_{\text{Th}} = (2.62 \pm 0.05) \times 10^{-2} \text{ d.p.m. m}^{-3} \text{ yr}^{-1}$; $\beta_{\text{Pa}}/\beta_{\text{Th}} = 0.093$; β , production rate; d.p.m., disintegrations per minute). Both are rapidly removed from sea water by adsorption on settling particles, resulting in relatively short residence times in the water column and in the accumulation of excess, or unsupported, ²³⁰Th and ²³¹Pa in the underlying sediments. ²³¹Pa is less rapidly removed than ²³⁰Th and has a residence time (~100–200 yr) approaching the transit time of deep water in the Atlantic basin³. As a result, approximately half of the ²³¹Pa produced in Atlantic water is exported with the North Atlantic Deep Water (NADW) into the Southern Ocean instead of being removed into the Atlantic sediments. On the other hand, ²³⁰Th has a shorter residence time (~20–40 yr), which minimizes its transport from the Atlantic to the Southern Ocean today. Modern North Atlantic sediments thus retain a mean $\text{ex}^{231}\text{Pa}_0/\text{ex}^{230}\text{Th}_0$ (excess ²³¹Pa and ²³⁰Th activity ratio decay-corrected to the time of deposition; ²³¹Pa/²³⁰Th hereafter) significantly lower than the seawater production ratio of 0.093. For a given scavenging rate, lower rates of meridional overturning circulation (MOC) in the past would result in comparatively less ²³¹Pa export from the Atlantic and in higher sedimentary ²³¹Pa/²³⁰Th, reaching a maximum of 0.093 for a total cessation^{4,5}.

In order to assess changes in MOC during the past 20 kyr, we have analysed a high-accumulation-rate core from Bermuda rise in the deep western subtropical Atlantic (OCE326-GGC5; 33° 42' N, 57° 35' W, 4.55 km). Deglacial stratigraphy was constructed using $\delta^{18}\text{O}$ measurements in individual shells of the planktonic foraminifera *Globorotalia inflata*, and the chronology was established using ¹⁴C dates from monospecific foraminifera samples. A large fraction

of Bermuda rise sediment consists of older fine-grained material laterally transported from the Canadian margin⁶. However, the kinetics of adsorption reactions are believed to be fast enough⁷ that the laterally transported sediment does not retain the ²³¹Pa/²³⁰Th from its initial site of deposition. Instead, ²³¹Pa/²³⁰Th is reset by equilibration with the transporting water, and the ²³¹Pa/²³⁰Th signal at the site of final deposition is synchronous with the deposition of the planktonic foraminifera that were used to establish the chronology. ²³⁰Th and ²³¹Pa were analysed by isotope dilution on a magnetic sector inductively coupled plasma mass spectrometer⁸.

The ²³¹Pa/²³⁰Th ratio in the most recent sediments (~0.055) is consistent with the export from the North Atlantic of ~10% of the ²³⁰Th and ~50% of the ²³¹Pa production by the vigorous modern MOC^{4,5}. Similar values characterize the entire Holocene sections (0.055 ± 0.006 ; 2σ ; $n = 9$), suggesting no major changes in Atlantic MOC during the past 10 kyr (Fig. 1). The slightly lower ratio (0.050) during the early Holocene implies a slightly increased rate of MOC, and a single higher ratio (0.062) in the mid-Holocene (~5 kyr ago) raises the possibility of a brief decline in MOC, but these results must be confirmed with additional high-resolution analyses.

The mean ²³¹Pa/²³⁰Th of sediment deposited during the Last Glacial Maximum (LGM) between 17.5 and 19.8 kyr ago (Fig. 1) is significantly higher (0.068 ± 0.010 ; 2σ ; $n = 12$) than during the Holocene (0.055 ± 0.006 ; 2σ ; $n = 9$). The difference in the mean ²³¹Pa/²³⁰Th between the Holocene and LGM ($\Delta(\text{ex}^{231}\text{Pa}/\text{ex}^{230}\text{Th})_{\text{LGM-Hol}} = 0.013 \pm 0.004$; 95% confidence interval) is at the upper limit of the range of glacial reduction in MOC estimated⁵ (30%) using a broader North Atlantic ²³¹Pa/²³⁰Th database and a circulation–biogeochemistry model. The new results from GGC5 also suggest no more than a ~30–40% slowdown of the MOC in the LGM, and probably less, because shallower overturning and generally higher glacial particle fluxes (Fig. 2) could also contribute to higher sedimentary ²³¹Pa/²³⁰Th.

In contrast, the deglaciation is marked by larger changes in ²³¹Pa/²³⁰Th whose timing suggests that rapid, large-scale oscillations in MOC occurred in concert with regional climatic variations

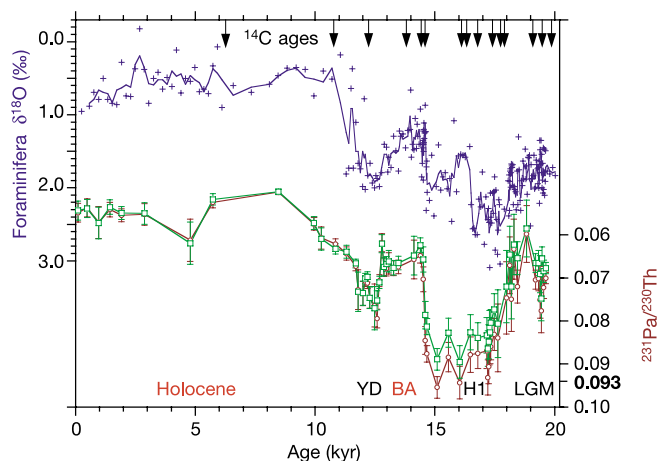


Figure 1 Stable isotope and radiochemical data from sediment core OCE326-GGC5 (33° 42' N, 57° 35' W, 4.55 km). Individual measurements and three-point running mean of planktonic foraminifera $\delta^{18}\text{O}$ (*G. inflata*) plotted with sedimentary ²³¹Pa/²³⁰Th against age (238-based values (red circles) are calculated by subtraction of supported ²³⁰Th and ²³¹Pa estimated from the measured ²³⁸U activity; 232-based values (green squares) are calculated by subtraction of supported ²³⁰Th and ²³¹Pa estimated from the measured ²³²Th activity $\times 0.57$ (see Methods)). Both $\delta^{18}\text{O}$ and ²³¹Pa/²³⁰Th axes are inverted. Arrows indicate ¹⁴C age control points. Labels above lower axis indicate significant climatic intervals: Holocene, warm; YD, Younger Dryas, cooling; BA, Bølling–Allerød, warm; H1, Heinrich event 1, iceberg discharge; LGM, Last Glacial Maximum.

(Fig. 2). The most striking feature of the $^{231}\text{Pa}/^{230}\text{Th}$ profile is the abrupt increase towards the production ratio of 0.093, starting at 17.5 kyr ago and continuing until 15 kyr ago. The data indicate a rapid decline in the export of ^{231}Pa from this site. As the response time of sediment $^{231}\text{Pa}/^{230}\text{Th}$ to changes in circulation is ~ 500 yr (refs 4, 5), the $^{231}\text{Pa}/^{230}\text{Th}$ profile can be interpreted as reflecting a quasi-total and nearly instantaneous cessation of the Atlantic MOC at 17.5 kyr ago. Higher $^{231}\text{Pa}/^{230}\text{Th}$ could also be produced by higher particle flux and/or higher opal concentration in settling particles,

reducing the residence time and fractionation of the two nuclides in the water column⁹. These alternative explanations can be ruled out, however, because clay and carbonate fluxes were lower than during the LGM, and Si/Al indicates that opal content in the sediment is negligible (Fig. 2) (see Methods section). The $^{231}\text{Pa}/^{230}\text{Th}$ signal is thus best interpreted as reflecting a nearly total shutdown of the MOC that lasted more than 2,000 yr.

The onset at 17.5 kyr ago coincides with the timing of Heinrich event H1^{10,11}, a catastrophic iceberg discharge into the North Atlantic, and with additional evidence for freshening at high latitudes¹², and diminished relative influence of northern-source deep waters during that time^{13,14}. Model simulations suggest that the MOC is sensitive to buoyancy forcing through surface salinity perturbations¹⁵, with a sufficiently marked response in some experiments to resemble a 'drop-dead circulation' with negligible over-turning¹⁶. It was previously tempting to speculate that the puzzling interval between the onset of the severe climate associated with the H1 iceberg catastrophe (~ 17 kyr ago) and the eventual dramatic warming¹⁷ of the Bølling–Allerød (~ 15 kyr ago) might be the result of such a drop-dead circulation¹⁸. The $^{231}\text{Pa}/^{230}\text{Th}$ results from GGC5 provide the best indication yet that such a scenario occurred during that time.

At the same time as the rise in $^{231}\text{Pa}/^{230}\text{Th}$, there is also an increase in planktonic foraminifera $\delta^{18}\text{O}$ (Fig. 2). The rapidity of the $\delta^{18}\text{O}$ shift and the fact that it occurs subsequent to the timing of the glacial maximum¹⁹ rule out the possibility that it reflects an increase in global ice volume. It must therefore represent a near-surface

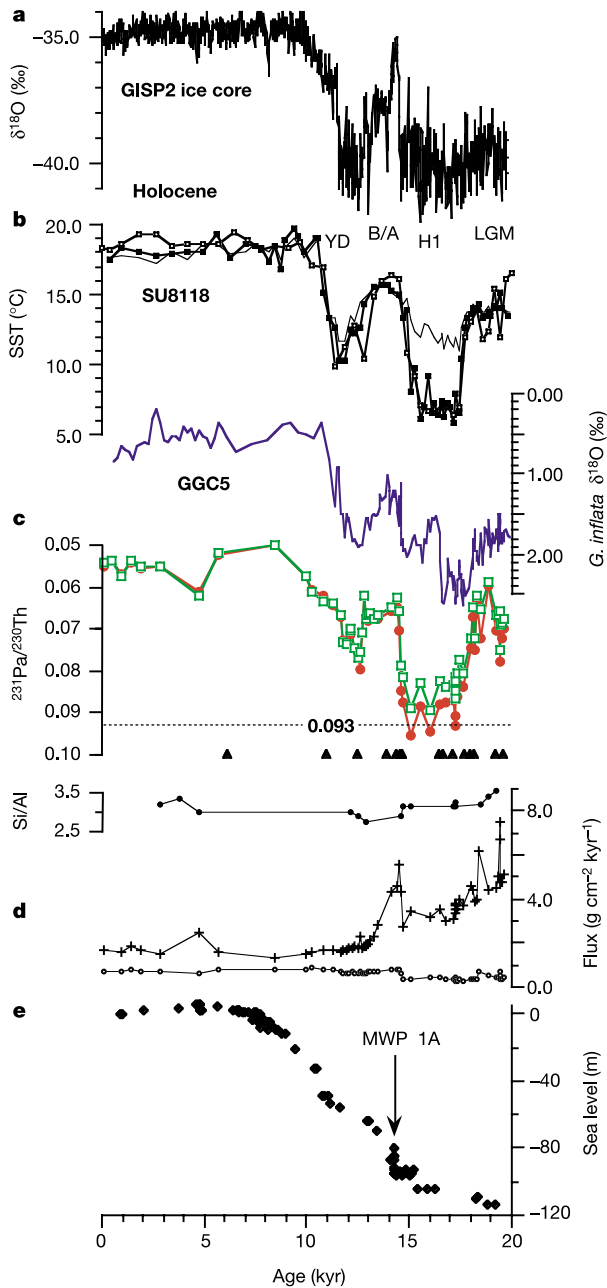


Figure 2 Comparison of sedimentary data from the subtropical Atlantic with ice-core, subpolar deep-sea core, and coral records for the past 20 kyr. **a**, Greenland $\delta^{18}\text{O}$ record²⁰. **b**, SST estimates from the subpolar North Atlantic based on planktonic foraminiferal assemblage²⁹ (open symbols) and two calibrations for alkenone unsaturation ratios¹¹. **c**, Three-point running mean of planktonic foraminifera $\delta^{18}\text{O}$ plotted with sedimentary $^{231}\text{Pa}/^{230}\text{Th}$ against calendar age in core GGC5. Black triangles indicate ^{14}C age control points. **d**, ^{230}Th -normalized fluxes of carbonate and terrigenous sediment. **e**, Sea-level rise due to melting ice sheets^{21,22}.

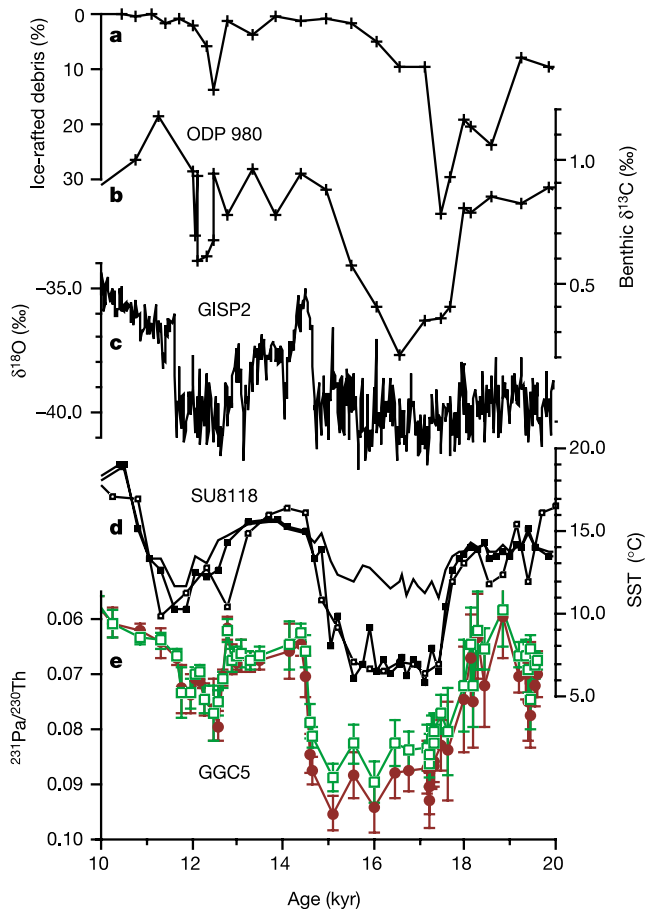


Figure 3 Deglacial records of ocean circulation and climate in the North Atlantic region. **a**, Ice-rafted debris record from ODP Site 980²⁵. **b**, Benthic foraminifera $\delta^{13}\text{C}$ from ODP Site 980²⁵. **c**, $\delta^{18}\text{O}$ in Greenland ice²⁰. **d**, SST estimates from the subpolar North Atlantic^{11,29}. **e**, Sedimentary $^{231}\text{Pa}/^{230}\text{Th}$ from GGC5.

cooling and/or increase in local salinity at the core location. The amplitude of the $\delta^{18}\text{O}$ increase (0.75–1.0‰) implies that sea surface temperature (SST) at this subtropical site may have been as much as 3–4 °C lower at the time of H1 than during the LGM. Minimum subpolar SST¹¹ and colder air temperatures over Greenland²⁰ are also evident at this time (Fig. 2), underscoring the fact that the LGM should not be viewed simply as a climatic extreme everywhere. The synchrony between changes in $^{231}\text{Pa}/^{230}\text{Th}$ and foraminifera $\delta^{18}\text{O}$ suggests a connection between the Atlantic MOC and local surface hydrography, and the inferred near-cessation of MOC during early deglaciation appears to be directly linked to the freshening and increased buoyancy of Northern Atlantic surface water^{10–12}. These findings thus support earlier suggestions that melt water associated with catastrophic iceberg discharge freshened the high-latitude surface ocean, stabilized the water column, and weakened the Atlantic MOC^{13,14,18}. Our results indicate that the effect was dramatic, resulting in a near-total collapse of the Atlantic MOC and substantial regional cooling.

The period of high $^{231}\text{Pa}/^{230}\text{Th}$ was terminated by a decrease to less than 0.065, suggesting an abrupt resumption of the Atlantic MOC at a time (~14.7 kyr ago) corresponding to the onset of the Bølling–Allerød warm period (Figs 1, 2). The timing of this resumption is shortly before the most rapid deglacial reduction of continental ice and sea-level rise, meltwater pulse 1a (MWP 1A), which has been dated at ~14.0 kyr ago^{21,22} (Figs 2, 3). Reinvigoration of the oceanic heat transport to high northern latitudes may have combined with increasing insolation to accelerate the melting of the Laurentide ice sheet, resulting in MWP 1A. Previous evidence has pointed to a large, rapid, high-latitude warming at this time^{17,23}. Our new results provide support for the idea that the rapidity and magnitude of this warming resulted in large part from the reinvigoration of the Atlantic MOC.

After reaching a minimum at 0.065 at 14.2 kyr ago, $^{231}\text{Pa}/^{230}\text{Th}$ remained nearly constant (0.065 ± 0.004 ; 2σ ; $n = 8$) for ~1,500 yr (14.2–12.5 kyr ago), when the temperature recorded in Greenland ice decreased in several steps (Fig. 3). This stepwise cooling, starting at ~14 kyr ago, does not seem to be the result of a decrease in the Atlantic MOC.

Melt water associated with H1 appears to have been particularly efficient at curtailing meridional overturning, most probably owing to the delivery of drifting icebergs closer to the sensitive locations of glacial deep-water formation. No equivalent suppression of MOC accompanied MWP 1A, even though this event may have involved much larger volumes of fresh water. One possible explanation is that this melt water originated primarily from Antarctica with only a modest contribution from the Northern Hemisphere²⁴. Another possibility is that runoff from the Laurentide ice sheet underwent substantial mixing with sea water before reaching the zones of deep convection. The site of deep-water production may also have migrated north of the Greenland–Iceland–Scotland ridge, farther from the influence of melt water from North America.

At 12.7 kyr ago, $^{231}\text{Pa}/^{230}\text{Th}$ increased abruptly, although not to the same level as during H1 (Fig. 2), but implying at least a partial reduction of the Atlantic MOC. This shift coincides with the beginning of the Younger Dryas, and is associated with an increase in the planktonic $\delta^{18}\text{O}$, probably reflecting a decrease in subtropical SST (Fig. 2). MWP 1A occurred too early to be a direct cause of a circulation change or cooling during the Younger Dryas. By contrast, evidence from the subpolar North Atlantic²⁵ points to a link between enhanced deposition of ice-rafted debris and a decline in $\delta^{13}\text{C}$ at this time (Fig. 3). The Younger Dryas may therefore have been triggered by iceberg discharge, in a manner similar to H1.

Unlike the earlier near-shutdown, however, the decline in MOC at 12.7 kyr ago did not last thousands of years. The rapid increase in $^{231}\text{Pa}/^{230}\text{Th}$ was immediately followed by decreases in both $\delta^{18}\text{O}$ and $^{231}\text{Pa}/^{230}\text{Th}$. This pattern may indicate a gradual re-acceleration of the Atlantic MOC, as suggested by the $\Delta^{14}\text{C}_{\text{atm}}$ reconstructed

from the Cariaco basin²⁶. In general, the $^{231}\text{Pa}/^{230}\text{Th}$ results are in agreement with $\Delta^{14}\text{C}_{\text{atm}}$ interpretations of deglacial changes in MOC, with a sharp decline during H1, a reinvigoration during the Bølling–Allerød to very similar values as the LGM, and then brief, sharp decline and gradual increase within the Younger Dryas and continuing into the Holocene^{26–28}.

At face value, the $^{231}\text{Pa}/^{230}\text{Th}$ suggests only a partial weakening of MOC during the Younger Dryas, in contrast to the near shutdown during H1. In this case, the comparison with estimated changes in SST^{11,29} suggests strong coupling between the Atlantic MOC and climate in at least part of the North Atlantic region for the past 20 kyr (Fig. 2). However, because of the brevity of the slowdown and the response time of $^{231}\text{Pa}/^{230}\text{Th}$ to circulation shutdowns (~500 yr), the Younger Dryas reduction in the rate of MOC may have been larger than indicated by the maximum in $^{231}\text{Pa}/^{230}\text{Th}$, and the possibility of a total, albeit very brief, shutdown cannot be ruled out.

The subsequent reinvigoration of the Atlantic MOC was more gradual than during the Bølling warming (Fig. 2), although lower sedimentation rates in this interval of GGC5 may have resulted in the smoothing of a more abrupt transition by bioturbation. Thereafter, the acceleration of the Atlantic MOC continued uninterrupted to its modern strength, which has largely prevailed throughout the Holocene. The deglacial transition thus contains the most dramatic changes in the rate of Atlantic MOC as well as the largest climatic oscillations of the past 20 kyr. Marked declines in MOC were associated with both the H1 and Younger Dryas millennial cooling events, and in each case the rapid subsequent increase in MOC was accompanied by abrupt warming. A remaining question is why the LGM reduction in MOC was limited to 30–40% or less, while briefer events were substantially larger. One possibility is that the steady-state rate of the overturning circulation may be fixed by the energy available for diapycnal mixing³⁰, whereas transient salinity perturbations at the surface may have a shorter-term but potentially more dramatic impact on MOC and its climatically significant heat transport. An improved understanding of the role of such transient perturbations should thus remain a high priority for future investigations. □

Methods

Uranium, thorium and protactinium were measured by isotope dilution on a Finnigan MAT Element 1 single collector, sector field, inductively coupled plasma mass spectrometer⁸. The samples were ground with mortar and pestle, then spiked with ^{233}Pa and ^{229}Th before total dissolution in HNO_3 , HF and HClO_4 . An aliquot of the resulting solution was removed, spiked with ^{236}U and ^{229}Th , and analysed for ^{238}U and ^{232}Th . The remaining solution was used for ^{231}Pa and ^{230}Th separation by ion-exchange chromatography. The internal precision on the measured $^{231}\text{Pa}/^{230}\text{Th}$ was usually better than 1.5% (2σ level). Reproducibility for full replicate analyses (dissolution, chromatographic separation and spectrometry) was usually better than 5% (2σ level) on the measured $^{231}\text{Pa}/^{230}\text{Th}$. Excess activities were obtained using two independent corrections for the supported detrital portion of the total ^{230}Th and ^{231}Pa measured. One estimate is based on the total ^{238}U activity and the other is based on the total ^{232}Th activity, using a $^{238}\text{U}/^{232}\text{Th}$ activity ratio (0.57) within a range typical for Atlantic sediment (0.6 ± 0.2)³⁵. Each estimate was corrected for radioactive decay of the unsupported nuclides since the time of sediment deposition determined from the ^{14}C -based age-model. The ^{238}U correction is sensitive to the deposition of authigenic U, and the ^{232}Th correction may be sensitive to variations in sediment source or type. The good agreement of the two estimates throughout the record (Fig. 1) indicates that these potentially confounding factors are not important here. Thus, no calculation of post-depositional ingrowth of ^{230}Th or ^{231}Pa from authigenic uranium was required.

Sedimentary fluxes

Mass fluxes were calculated from the decay-corrected activity of excess ^{230}Th per gram of sediment and the expected ^{230}Th flux to the sea floor, given the concentration of ^{234}U in sea water and the water depth³². Fluxes of CaCO_3 and terrigenous sediment of all sizes were calculated based on the bulk mass flux and the percentage of CaCO_3 , measured by coulometer. Uncertainties in the mass flux estimates averaged <6%. Two other sediment types, authigenic precipitates and opal, occurred in negligible amounts, although the potential influence of opal on $^{231}\text{Pa}/^{230}\text{Th}$ led us to explore several means of assessing its presence. Bulk Si/Al (Fig. 2) measured on a representative sample set (3.1 ± 0.2) was found to be slightly below that of the upper continental crust (3.8) and similar to the average post-Archaean Australian terrigenous shale (2.9). Fine-fraction aliquots were prepared for micropalaeontological analysis of diatoms and examined with a compound

light microscope, but too few frustules occurred to allow quantification. The coarse, sand-sized fraction of the samples was also examined visually. In particular, the sediments greater than 150 μm , representing less than 1% of the sample weight, were examined for large diatoms in the deglacial interval of the core. A portion of these samples contained the diatom *Ethmodiscus rex*, although their occurrence does not covary with $^{231}\text{Pa}/^{230}\text{Th}$, and none were observed from 190–220 cm, when $^{231}\text{Pa}/^{230}\text{Th}$ reached maximum values. Although it cannot be entirely ruled out that additional diatom frustules or other opal may have been deposited originally and subsequently dissolved, the described analyses indicate that opal concentration in the sediments is negligible and cannot account for the $^{231}\text{Pa}/^{230}\text{Th}$ signal.

Stratigraphy and chronology

The stratigraphy for the core was constructed using $\delta^{18}\text{O}$ measurements on single shells of the planktonic foraminifera *G. inflata*. Samples of 0.5–1.0 cm thickness were taken from the core and dried. The dry samples were weighed, immersed in distilled water, and wet-sieved using a 63- μm mesh. The >63- μm fraction was dried again, and dry-sieved using a 150- μm mesh. Individual specimens of *G. inflata* were hand-selected from the >150- μm fraction using 25–50 \times magnification under a binocular microscope. Each specimen was acidified and analysed on a partially automated VG 903 stable isotope mass spectrometer. The resulting oxygen isotope ratios were calibrated to $\delta^{18}\text{O}$ using NBS-19 and are reported relative to the Pee Dee Belemnite (PDB) standard. A chronology for the core was established using fourteen ^{14}C dates from monospecific foraminifera samples (typically *G. inflata*). An abundance maximum of dextral coiling *Neogloboquadrina pachyderma* was used to obtain a date for the Younger Dryas interval, and in one case *Globigerinoides ruber* was measured for ^{14}C along with *G. inflata*. The age difference between the two species is less than the measurement uncertainty. A reservoir correction of 400 yr was applied to the measured ^{14}C , and the ages were converted to calendar years using the CALIB 4.3 calibration program³³.

Received 2 January; accepted 16 March 2004; doi:10.1038/nature02494.

1. Boyle, E. A. & Keigwin, L. North Atlantic thermohaline circulation during the past 20,000 years linked to high-latitude surface temperature. *Nature* **330**, 35–40 (1987).
2. Legrand, P. & Wunsch, C. Constraints from paleotracer data on the North Atlantic circulation during the last glacial maximum. *Paleoceanography* **10**, 1011–1045 (1995).
3. Broecker, W. S. A revised estimate of the radiocarbon age of the North Atlantic Deep Water. *J. Geophys. Res.* **84**, 3218–3226 (1979).
4. Yu, E.-F., Francois, R. & Bacon, M. P. Similar rates of modern and last-glacial ocean thermohaline circulation inferred from radiochemical data. *Nature* **379**, 689–694 (1996).
5. Marchal, O., Francois, R., Stocker, T. F. & Joos, F. Ocean thermohaline circulation and sedimentary $^{231}\text{Pa}/^{230}\text{Th}$ ratio. *Paleoceanography* **15**, 625–641 (2000).
6. Ohkouchi, N., Eglinton, T. L., Keigwin, L. D. & Hayes, J. M. Spatial and temporal offsets between proxy records in a sediment drift. *Science* **298**, 1224–1227 (2002).
7. Bacon, M. P. & Anderson, R. F. Distribution of thorium isotopes between dissolved and particulate forms in the deep sea. *J. Geophys. Res.* **87**, 2045–2056 (1982).
8. Choi, M.-S. *et al.* Rapid determination of ^{230}Th and ^{231}Pa in seawater by desolvated-micronebulization inductively-coupled magnetic sector mass spectrometry. *Mar. Chem.* **76**, 99–112 (2001).
9. Chase, Z., Anderson, R. F., Fleisher, M. Q. & Kubik, P. W. The influence of particle composition and particle flux on scavenging of Th, Pa and Be in the ocean. *Earth Planet. Sci. Lett.* **204**, 215–229 (2002).
10. Bond, G. *et al.* Evidence for massive discharge of icebergs into the glacial Northern Atlantic. *Nature* **360**, 245–249 (1992).
11. Bard, E., Rostek, F., Turon, J.-L. & Gendreau, S. Hydrological impact of Heinrich Events in the Subtropical Northeast Atlantic. *Science* **289**, 1321–1323 (2000).
12. Duplessy, J.-C. *et al.* Changes in surface salinity of the North Atlantic Ocean during the last deglaciation. *Nature* **358**, 485–488 (1993).
13. Vidal, L. *et al.* Evidence for changes in the North Atlantic Deep Water linked to meltwater surges during the Heinrich events. *Earth Planet. Sci. Lett.* **146**, 13–27 (1997).
14. Eliot, M., Labeyrie, L. & Duplessy, J.-C. Changes in North Atlantic deep-water formation associated with the Dansgaard-Oeschger temperature oscillations (60–10 ka). *Quat. Sci. Rev.* **21**, 1153–1165 (2002).
15. Rahmstorf, S. Bifurcations of the Atlantic thermohaline circulation in response to changes in the hydrological cycle. *Nature* **378**, 145–149 (1995).
16. Manabe, S. & Stouffer, R. J. Two stable equilibria of a coupled ocean-atmosphere model. *J. Clim.* **1**, 841–866 (1988).
17. Severinghaus, J. P. & Brook, E. J. Abrupt climate change at the end of the last glacial period inferred from trapped air in polar ice. *Science* **286**, 930–934 (1999).
18. Broecker, W. S. Massive iceberg discharges as triggers for global climate change. *Nature* **372**, 421–424 (1994).
19. Mix, A. C., Bard, E. & Schneider, R. Environmental processes of the ice age: Land, oceans, glaciers (EPILOG). *Quat. Sci. Rev.* **20**, 627–657 (2001).
20. Grootes, P. M., Stuiver, M., White, J. W. C., Johnsen, S. & Jouzel, J. Comparison of oxygen isotope records from the GISP2 and GRIP Greenland ice cores. *Nature* **366**, 552–554 (1993).
21. Fairbanks, R. G. A 17,000-year glacio-eustatic sea level record: influence of glacial melting rates on the Younger Dryas event and deep-ocean circulation. *Nature* **342**, 637–642 (1989).
22. Bard, E. *et al.* Deglacial sea-level record from Tahiti corals and the timing of global meltwater discharge. *Nature* **382**, 241–244 (1996).
23. Lehman, S. J. & Keigwin, L. D. Sudden changes in North Atlantic circulation during the last deglaciation. *Nature* **356**, 757–762 (1992).
24. Clark, P. U., Mitrovic, J. X., Milne, G. A. & Tamiseia, M. E. Sea-level fingerprinting as a direct test for the source of global meltwater pulse 1A. *Science* **295**, 2438–2441 (2002).
25. McManus, J. F., Oppo, D. W. & Cullen, J. L. A 0.5 million year record of millennial-scale climate variability in the North Atlantic. *Science* **283**, 971–975 (1999).
26. Hughen, K. A. *et al.* Deglacial changes in ocean circulation from an extended radiocarbon calibration. *Nature* **391**, 65–68 (1998).

27. Clark, P. U., Pisias, N. G., Stocker, T. & Weaver, A. The role of the thermohaline circulation in abrupt climate change. *Nature* **415**, 863–869 (2002).
28. Hughen, K. A. *et al.* ^{14}C Activity and global carbon cycle changes over the past 50,000 years. *Science* **303**, 202–207 (2004).
29. Waelbroeck, C. *et al.* Improving past sea surface temperature estimates based on planktonic fossil faunas. *Paleoceanography* **13**, 272–283 (1998).
30. Munk, W. & Wunsch, C. Abyssal recipes II: energetics of tidal and wind mixing. *Deep-Sea Res.* **145**, 1976–2009 (1998).
31. McManus, J. F., Anderson, R. F., Broecker, W. S., Fleisher, M. Q. & Higgins, S. M. Radiometrically determined fluxes in the sub-polar North Atlantic during the last 140,000 years. *Earth Planet. Sci. Lett.* **135**, 29–43 (1998).
32. Francois, R., Frank, M., Rutgers van der Loeff, M. M. & Bacon, M. P. ^{230}Th -normalization: An essential tool for interpreting sedimentary fluxes during the late Quaternary. *Paleoceanography* **19**, doi:10.1029/2003PA000939 (2004).
33. Stuiver, M. *et al.* INTCAL98 radiocarbon age calibration. *Radiocarbon* **40**, 1041–1083 (1998).

Supplementary Information accompanies the paper on www.nature.com/nature.

Acknowledgements This study was improved by assistance and input from O. Marchal, M. Bacon, W. Curry, L. Labeyrie, R. Anderson, N. Ohkouchi and T. Eglinton. Technical expertise was provided by A. Fleer, E. Roosen, L. Zou, S. Manganini, E. Frank, L. Ball, D. Schneider, I. Grigorov, S. Benetti, M. Jęglinski and A. Edwards. Support for this research was provided in part by the US-NSF OCE and INT programmes, the France CNRS, WHOI-OCCI and Mellon awards, and the Comer Science and Education Foundation.

Competing interests statement The authors declare that they have no competing financial interests.

Correspondence and requests for materials should be addressed to J.F.M. (jmcmans@whoi.edu).

.....

Dislocation creep in MgSiO₃ perovskite at conditions of the Earth’s uppermost lower mantle

Patrick Cordier^{1,2}, Tamás Ungár³, Lehel Zsoldos³ & Géza Tichy⁴

¹Laboratoire de Structure et Propriétés de l’Etat Solide, UMR CNRS 8008, Université des Sciences et Technologies de Lille, F-59655 Villeneuve d’Ascq Cedex, France

²Bayerisches Geoinstitut, Universität Bayreuth, D-95440 Bayreuth, Germany

³Department of General Physics,

⁴Department of Solid State Physics, Eötvös University Budapest, H-1518 POB 32, Budapest, Hungary

.....

Seismic anisotropy provides an important observational constraint on flow in the Earth’s deep interior. The quantitative interpretation of anisotropy, however, requires knowledge of the slip geometry of the constitutive minerals that are responsible for producing rock fabrics. The Earth’s lower mantle is mostly composed of (Mg, Fe)SiO₃ perovskite¹, but as MgSiO₃ perovskite is not stable at high temperature under ambient pressure, it has not been possible to investigate its mechanical behaviour with conventional laboratory deformation experiments. To overcome this limitation, several attempts were made to infer the mechanical properties of MgSiO₃ perovskite on the basis of analogue materials^{2–7}. But perovskites do not constitute an analogue series for plastic deformation, and therefore the direct investigation of MgSiO₃ perovskite is necessary. Here we have taken advantage of recent advances in experimental high-pressure rheology⁸ to perform deformation experiments on coarse-grained MgSiO₃ polycrystals under pressure and temperature conditions of the uppermost lower mantle. We show that X-ray peak broadening measurements developed in metallurgy can be adapted to low-symmetry minerals to identify the elementary deformation mechanisms activated under these conditions. We conclude that, under uppermost lower-mantle conditions, MgSiO₃ perovskite